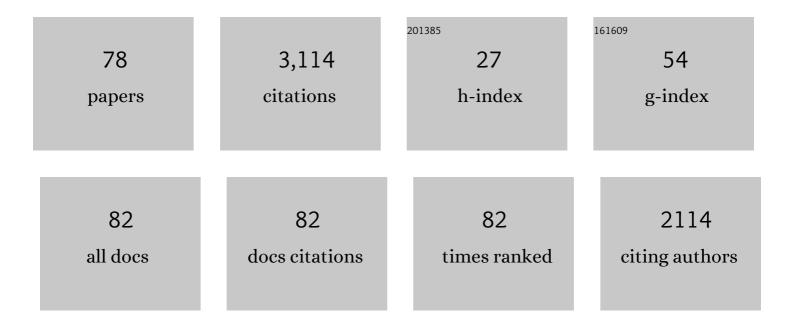
William A Brantley

List of Publications by Year in descending order

Source: https://exaly.com/author-pdf/2841565/publications.pdf Version: 2024-02-01



#	Article	IF	CITATIONS
1	An initial investigation of the bending and torsional properties of nitinol root canal files. Journal of Endodontics, 1988, 14, 346-351.	1.4	861
2	SEM Observations of Nickel-Titanium Rotary Endodontic Instruments that Fractured During Clinical Use. Journal of Endodontics, 2005, 31, 40-43.	1.4	214
3	Metallurgical Characterization of a New Nickel-Titanium Wire for Rotary Endodontic Instruments. Journal of Endodontics, 2009, 35, 1589-1593.	1.4	173
4	A Three-Dimensional Finite Element Stress Analysis of Angled Abutments for an Implant Placed in the Anterior Maxilla. Journal of Prosthodontics, 1995, 4, 95-100.	1.7	87
5	Electrochemical characteristics of nanotubes formed on Ti–Nb alloys. Thin Solid Films, 2009, 517, 5038-5043.	0.8	84
6	Differential scanning calorimetry (DSC) analyses of superelastic and nonsuperelastic nickel-titanium orthodontic wires. American Journal of Orthodontics and Dentofacial Orthopedics, 1996, 109, 589-597.	0.8	83
7	Bending properties of superelastic and nonsuperelastic nickel-titanium orthodontic wires. American Journal of Orthodontics and Dentofacial Orthopedics, 1991, 99, 310-318.	0.8	75
8	Comparison of bending and tension tests for orthodontic wires. American Journal of Orthodontics, 1986, 89, 228-236.	0.4	73
9	Nanotube morphology changes for Ti–Zr alloys as Zr content increases. Thin Solid Films, 2009, 517, 5033-5037.	0.8	64
10	Effect of coating on properties of esthetic orthodontic nickel-titanium wires. Angle Orthodontist, 2012, 82, 319-325.	1.1	62
11	Nanotubular oxide layer formation on Ti–13Nb–13Zr alloy as a function of applied potential. Journal of Materials Science, 2009, 44, 3975-3982.	1.7	56
12	Porcelain adherence vs force to failure for palladium–gallium alloys: a critique of metal–ceramic bond testing. Dental Materials, 1998, 14, 112-119.	1.6	54
13	Temperature-modulated DSC provides new insight about nickel-titanium wire transformations. American Journal of Orthodontics and Dentofacial Orthopedics, 2003, 124, 387-394.	0.8	47
14	Effects of a diamond-like carbon coating on the frictional properties of orthodontic wires. Angle Orthodontist, 2011, 81, 141-148.	1.1	46
15	Micro-XRD and temperature-modulated DSC investigation of nickel–titanium rotary endodontic instruments. Dental Materials, 2009, 25, 1221-1229.	1.6	45
16	Porcelain adherence to high-palladium alloys. Journal of Prosthetic Dentistry, 1993, 70, 386-394.	1.1	44
17	Comparisons of nanoindentation, 3-point bending, and tension tests for orthodontic wires. American Journal of Orthodontics and Dentofacial Orthopedics, 2011, 140, 65-71.	0.8	44
18	Cobalt-Chromium and Nickel-Chromium Alloys for Removable Prosthodontics, Part 1: Mechanical Properties. Journal of Prosthodontics, 1993, 2, 144-150.	1.7	38

#	Article	IF	CITATIONS
19	Metallurgical Structure and Microhardness of Four New Palladium-Based Alloys. Journal of Prosthodontics, 1996, 5, 288-294.	1.7	38
20	Hydroxyapatite thin film coatings on nanotube-formed Ti–35Nb–10Zr alloys after femtosecond laser texturing. Surface and Coatings Technology, 2013, 217, 13-22.	2.2	35
21	InÂvitro fit of CAD-CAM complete arch screw-retained titanium and zirconia implant prostheses fabricated on 4 implants. Journal of Prosthetic Dentistry, 2018, 119, 409-416.	1.1	34
22	X-ray diffraction studies of oxidized high-palladium alloys. Dental Materials, 1996, 12, 333-341.	1.6	30
23	Nanostructured thin film formation on femtosecond laser-textured Ti–35Nb–xZr alloy for biomedical applications. Thin Solid Films, 2011, 519, 4668-4675.	0.8	29
24	Electrochemical and surface behavior of hydyroxyapatite/Ti film on nanotubular Ti–35Nb–xZr alloys. Applied Surface Science, 2012, 258, 2129-2136.	3.1	29
25	Hydroxyapatite precipitation on nanotubular films formed on Ti-6Al-4V alloy for biomedical applications. Thin Solid Films, 2013, 549, 135-140.	0.8	29
26	Morphology of hydroxyapatite nanoparticles in coatings on nanotube-formed Ti–Nb–Zr alloys for dental implants. Vacuum, 2014, 107, 297-303.	1.6	29
27	Formation of titanium dioxide nanotubes on Ti–30Nb–xTa alloys by anodizing. Thin Solid Films, 2013, 549, 141-146.	0.8	27
28	Hydroxyapatite formation on biomedical Ti–Ta–Zr alloys by magnetron sputtering and electrochemical deposition. Thin Solid Films, 2014, 572, 119-125.	0.8	27
29	Potentiodynamic polarization study of the in vitro corrosion behavior of 3 high-palladium alloys and a gold-palladium alloy in 5 media. Journal of Prosthetic Dentistry, 2002, 87, 86-93.	1.1	26
30	Effects of bonding materials on the mechanical properties of enamel around orthodontic brackets. Angle Orthodontist, 2012, 82, 187-195.	1.1	26
31	Studies of orthodontic elastomeric modules. Part 1: Glass transition temperatures for representative pigmented products in the as-received condition and after orthodontic use. American Journal of Orthodontics and Dentofacial Orthopedics, 2004, 126, 337-343.	0.8	25
32	X-ray diffraction studies of as-cast high-palladium alloys. Dental Materials, 1995, 11, 154-160.	1.6	24
33	Evaluation of high-temperature distortion of high-palladium metal-ceramic crowns. Journal of Prosthetic Dentistry, 2001, 85, 133-140.	1.1	24
34	The measure of wear inN-vinyl pyrrolidinone (NVP) modifed glass-ionomer cements. Polymers for Advanced Technologies, 2005, 16, 113-116.	1.6	24
35	Microstructural studies of 35°C Copper Ni–Ti orthodontic wire and TEM confirmation of low-temperature martensite transformation. Dental Materials, 2008, 24, 204-210.	1.6	24
36	Inductively coupled plasma-mass spectroscopy measurements of elemental release from 2 high-palladium dental casting alloys into a corrosion testing medium. Journal of Prosthetic Dentistry, 2002, 87, 80-85.	1.1	23

#	Article	IF	CITATIONS
37	Hydroxyapatite coating on micropore-formed titanium alloy utilizing electrochemical deposition. Thin Solid Films, 2013, 549, 154-158.	0.8	23
38	Surface characteristics of hydroxyapatite films deposited on anodized titanium by an electrochemical method. Thin Solid Films, 2013, 546, 185-188.	0.8	21
39	Torsional and metallurgical properties of rotary endodontic instruments. II. Stainless steel Gates Glidden drills. Journal of Endodontics, 1991, 17, 319-323.	1.4	20
40	Differential scanning calorimetry (DSC) and temperature-modulated DSC study of three mouthguard materialsa~†. Dental Materials, 2007, 23, 1492-1499.	1.6	20
41	Evolution, clinical applications, and prospects of nickel-titanium alloys for orthodontic purposes. Journal of the World Federation of Orthodontists, 2020, 9, S19-S26.	0.9	20
42	Vickers Hardness Investigation of Work-Hardening in Used NiTi Rotary Instruments. Journal of Endodontics, 2006, 32, 1191-1193.	1.4	19
43	Effect of mechanical properties of fillers on the grindability of composite resin adhesives. American Journal of Orthodontics and Dentofacial Orthopedics, 2010, 138, 420-426.	0.8	19
44	Effect of different high-palladium metal-ceramic alloys on the color of opaque porcelain. Journal of Prosthodontics, 2000, 9, 71-76.	1.7	18
45	Phenomena of Nanotube Nucleation and Growth on New Ternary Titanium Alloys. Journal of Nanoscience and Nanotechnology, 2010, 10, 4684-4689.	0.9	18
46	Mechanical properties, fracture surface characterization, and microstructural analysis of six noble dental casting alloys. Journal of Prosthetic Dentistry, 2011, 105, 394-402.	1.1	18
47	Silicon-substituted hydroxyapatite coating with Si content on the nanotube-formed Ti–Nb–Zr alloy using electron beam-physical vapor deposition. Thin Solid Films, 2013, 546, 189-195.	0.8	18
48	Hydroxyapatite deposition on micropore-formed Ti-Ta-Nb alloys by plasma electrolytic oxidation for dental applications. Surface and Coatings Technology, 2016, 294, 15-20.	2.2	18
49	Fracture analysis of monolithic CAD AM crowns. Journal of Esthetic and Restorative Dentistry, 2019, 31, 346-352.	1.8	17
50	Electrochemically-coated hydroxyapatite films on nanotubular Ti Nb alloys prepared in solutions containing Ca, P, and Zn ions. Thin Solid Films, 2016, 620, 132-138.	0.8	15
51	Potentiodynamic polarization study of the corrosion behavior of palladium-silver dental alloys. Journal of Prosthetic Dentistry, 2018, 119, 650-656.	1.1	15
52	A load-to-fracture and strain analysis of monolithic zirconia cantilevered frameworks. Journal of Prosthetic Dentistry, 2017, 118, 752-758.	1.1	14
53	Transmission electron microscopic investigation of high-palladium dental casting alloys. Dental Materials, 1997, 13, 365-371.	1.6	13
54	Surface characteristics of hydroxyapatite coatings on nanotubular Ti–25Ta–xZr alloys prepared by electrochemical deposition. Surface and Coatings Technology, 2014, 259, 274-280.	2.2	13

#	Article	IF	CITATIONS
55	Comparison of the metal-to-ceramic bondÂstrengths of four noble alloys withÂpress-on-metal and conventional porcelain layering techniques. Journal of Prosthetic Dentistry, 2014, 112, 1194-1200.	1.1	12
56	Hydroxyapatite-silicon film deposited on Ti–Nb–10Zr by electrochemical and magnetron sputtering method. Thin Solid Films, 2016, 620, 114-118.	0.8	12
57	The effect of metal recasting on porcelain-metal bonding: A force-to-failure study. Journal of Prosthetic Dentistry, 2010, 104, 165-172.	1.1	11
58	Surface morphology of TiN-coated nanotubular Ti–25Ta–xZr alloys for dental implants prepared by RF sputtering. Thin Solid Films, 2013, 549, 131-134.	0.8	11
59	Surface morphology of Zn-containing hydroxyapatite (Zn-HA) deposited electrochemically on Ti–xNb alloys. Thin Solid Films, 2015, 587, 163-168.	0.8	11
60	Viscoelastic properties of elastomeric chains: An investigation of pigment and manufacturing effects. American Journal of Orthodontics and Dentofacial Orthopedics, 2012, 141, 315-326.	0.8	10
61	Differences between buccal and lingual bone quality and quantity of peri-implant regions. Journal of the Mechanical Behavior of Biomedical Materials, 2016, 60, 48-55.	1.5	9
62	Distortion of CAD-CAM-fabricated implant-fixed titanium and zirconia complete dental prosthesis frameworks. Journal of Prosthetic Dentistry, 2018, 119, 116-123.	1.1	9
63	Comparison of 3D displacements of screw-retained zirconia implant crowns into implants with different internal connections with respect to screw tightening. Journal of Prosthetic Dentistry, 2018, 119, 132-137.	1.1	8
64	Electrochemical impedance spectroscopy study of corrosion characteristics of palladium–silver dental alloys. Journal of Biomedical Materials Research - Part B Applied Biomaterials, 2021, 109, 1777-1786.	1.6	7
65	Adhesion testing of a denture base resin with 5 casting alloys. Journal of Prosthodontics, 2000, 9, 30-36.	1.7	6
66	Fatigue limits and SEM/TEM observations of fracture characteristics for three Pd—Ag dental casting alloys. Journal of Materials Science: Materials in Medicine, 2007, 18, 119-125.	1.7	4
67	Hydroxyapatite Precipitation on Nanotube Surfaces of Ti–35Ta– <i>x</i> Nb Alloys. Journal of Nanoscience and Nanotechnology, 2014, 14, 7581-7584.	0.9	4
68	Highly ordered nanotubular film formation on Ti–25Nb–xZr and Ti–25Ta–xHf. Thin Solid Films, 2015, 596, 94-100.	0.8	4
69	Reprint of "Hydroxyapatite deposition on micropore-formed Ti-Ta-Nb alloys by plasma electrolytic oxidation for dental applications― Surface and Coatings Technology, 2016, 307, 1152-1157.	2.2	4
70	Wear characteristics and inhibition of enamel demineralization by resinâ€based coating materials. European Journal of Oral Sciences, 2017, 125, 160-167.	0.7	3
71	A study of fracture loads and fracture characteristics of teeth. Journal of Advanced Prosthodontics, 2019, 11, 187.	1.1	3
72	ICP-MS measurements of elemental release from two palladium alloys into a corrosion testing medium for different solution volumes and agitation conditions. Journal of Prosthetic Dentistry, 2021, , .	1.1	3

#	Article	IF	CITATIONS
73	Novel sensor to investigate microstructural contributions to corrosion of highâ€palladium dental alloys. Medical Devices & Sensors, 2020, 3, e10060.	2.7	2
74	SEM study of simulated clinical use for four nickel–titanium rotary endodontic files. Medical Devices & Sensors, 2019, 2, e10024.	2.7	1
75	Idealized force decay of orthodontic elastomeric chains follows Nutting Equation. Medical Devices & Sensors, 2021, 4, e10145.	2.7	1
76	Metallurgical Characterization of Laser-Sintered Cobalt-Chromium Dental Alloy. Ceramic Transactions, 2014, , 11-20.	0.1	0
77	Microâ€XRD and nanoindentation investigation of bioceramics for dental pulp therapy. Medical Devices & Sensors, 2019, 2, e10027.	2.7	0
78	Nonlinear sensors for biomaterials—Principles and applications. Medical Devices & Sensors, 2020, 3, e10101.	2.7	0